

Study on Motion Sensing Using Textile Electrodes-Focusing on the Application of PANI Conductive Material

Chenlu Wang^{1,2,3}, Hayoung Song^{3*}

¹ College of Textile and Apparel, Shaoxing University, Shaoxing, Zhejiang, 312000, China

² Key Laboratory of Clean Dyeing and Finishing Technology of Zhejiang Province, Shaoxing University, Shaoxing, Zhejiang, 312000, China

³ Department of Textile Design, Sangmyung University, Korea

* Corresponding author. E-mail: fabricsong@smu.ac.kr

Abstract

This study investigates the application of textile electrodes using PANI (Polyaniline) conductive material for motion sensing, specifically aimed at motion monitoring for the elderly. By depositing a PANI conductive layer on the base of warp-knitted fabric through in-situ polymerization and plasma treatment, a PCCWKF (Polyaniline Coated Conductive Warp-Knitted Fabric) with enhanced electrical conductivity and mechanical flexibility was developed. The research optimized the electrical resistivity and durability of PCCWKF by incorporating Polyvinyl Alcohol (PVA) as a toughening agent, improving the adhesion of the PANI conductive layer to the textile substrate. The sensor's efficacy in accurately recording and monitoring motion amplitude and frequency in real-time was demonstrated through its application in smart clothing, focusing on respiratory, elbow, and knee motion monitoring. This study holds significant implications for the advancement of wearable technology and smart textiles in the health monitoring of the elderly.

Keywords

PANI, conductive material, motion monitoring.

Since the 1930s, people have synthesized a variety of synthetic organic polymer materials with high strength, light weight and easy processing [1]. These materials have greatly impacted the production and lifestyle of humans, among which polymer materials such as polyamide and polyester have caused a revolution in the fiber and textile industries [2]. However, it is well known that these materials are poor conductors of electricity and fail to play a role in important applications such as conductive, electronic and magnetic materials. In 1974, in the laboratory of Hideki Shirakawa, a professor at the University of Tsukuba, Japan, polyacetylene (PA) was unexpectedly synthesized with alternating single and double bonds under high catalyst concentration [3]. Subsequently, Shirakawa, Alan J. Heeger and Alan G. MacDiarmid [4], polymer chemists at the University of Pennsylvania, United States, cooperated and found that when PA film was doped with AsF₅ or I₂, its electrical conductivity increased by 109 times, showing obvious metallic characteristics. This study not only ended the traditional concept of polymer materials as insulators but also played an important role in the basic theoretical research of organic polymers, ultimately promoting the establishment and

development of molecular and solid ion conductive theories.

The discovery of conductive PA has ushered in a new era of extensive research for inherently conductive polymers (ICPs). In the following years, researchers found a number of π -bonded polymers, such as polypyrrole, polyphenylacetylene, polythiophene, and PANI conjugated structural polymer materials, that show conductive properties after doping, and the electrical conductivity can reach the level of semiconductors or even metal conductors.

Among the conductive polymers above, PANI is considered to be the most promising one for practical application. In fact, in the late 1960s, Jozefowicz et al [5], used ammonium persulfate as an oxidant to prepare PANI with a conductivity of 10 S/cm. They found that PANI had proton exchange, oxidation-reduction (REDOX) and water vapor adsorption properties and used PANI as an electrode to assemble a secondary battery. However, the findings went unnoticed at that time.

In the mid-1980s, the research of MacDiarmid et al. led to a new understanding and great interest in PANI. PANI is a conductive polymer material with a π -bond conjugated structure.

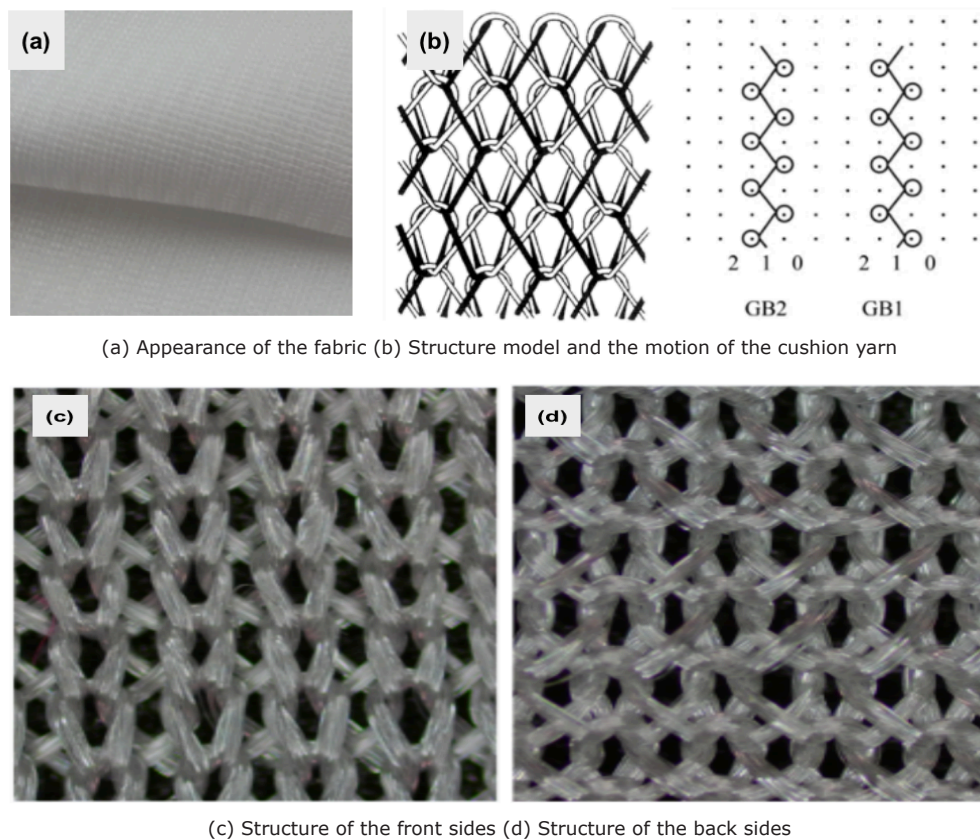
Compared with other conductive polymers, PANI has the advantages of a unique doping phenomenon, low cost, simple synthesis, good electrochemical reversibility, conductivity and stability [6], making it the most promising. In 1987, the button secondary battery, consisting of a PANI electrode, entered the market as a commodity, and PANI soon became the research hotspot in the field of conductive polymers [7]. At present, PANI has been widely used in many fields, such as anti-static, electromagnetic shielding, and anti-corrosion applications, and in many products, such as sensors, electrochromic materials, rechargeable batteries, biosensors and molecular circuits, spanning the electronics, microelectronics and chemical industries.

1. Preparation of Polyaniline Coated Conductive Warp-Knitted Fabric (PCCWKF)

PCCWKF, the full name of which is PANI coated conductive warp-knitted fabric, is a warp-knitted fabric formed on a polyester fiber base. After the method of in-situ polymerization, the PANI conductive layer was deposited on the warp-knitted fabric. The fabric has obvious electrical conductivity.

Raw Material	Structure	Weight/g·m ⁻²	PB·5 cm ⁻¹	PA·5 cm ⁻¹	Thickness/mm
Polyester	Two Bar Tricot Stitch	75	87	80	0.3

Table 1. Warp-knitted fabric specifications for experimental use



(a) Appearance of the fabric (b) Structure model and the motion of the cushion yarn

(c) Structure of the front sides (d) Structure of the back sides

Fig. 1. Basic information of two-comb warp-knitted fabric

The material is polyester with a double-warp flat structure. The double-warp flat fabric is the simplest double-comb structured warp-knitted fabric. It has the characteristics of thinness, soft properties, upright coils, uniform appearance, clear lines, and good lateral extension and resilience. It is the ideal base material for flexible wearable sensors. Table 1 shows the specifications of the fabric after finishing.

The appearance of the fabric is shown in Figure 1(a). The structure model and the motion of the cushion yarn are shown in Figure 1(b). The structures of the front and back sides are shown in Figure 1(c) and (d). The fabric is woven with two comb bars, both of which are woven with a flat structure. The cushion yarn moves in the opposite direction (in the figure below, the black yarn in the figure is the front comb yarn, and the white yarn is

the back comb yarn). The numbers of the cushion yarn are as follows: front comb GB1: 1-0/1-2// and back comb GB2: 1-2/1-0//.

PANI is an organic polymer with a π -conjugated structure, which has high rigidity but poor flexibility. When the PANI conductive layer on the fiber surface is affected by an external force, it is prone to show brittle fractures, which interrupts the conductive channel and reduces the conductive property. At the same time, the physical combination between the fiber surface and PANI generally has a low fastening capability, resulting in damage to part of the PANI conductive layer, which tends to easily separate and fall from the fiber surface. It does not have the ability of long-term fixation and has difficulty withstanding various external forces during fiber processing and product use.

Therefore, it cannot truly be applied. Aiming at this problem, researchers have used various methods, including chromic acid etching, alkali decrement treatment [8], and a modified epoxy group [9], to improve the surface ability of the fiber. There is, to some extent, a positive effect on enhancing the fastening between PANI and matrix fibers and improving the conductivity and durability of the composite conductive fiber. However, this cannot radically solve the problem of the low conductive layer flexibility. To improve the flexibility of PANI, other polymers such as polyvinyl alcohol (PVA) and PANI are used as composite thin films [10]. The presence of PVA increased the elongation at break from approximately 2% to more than 40%, indicating that the presence of PVA has a positive effect on improving the flexibility of the PANI conductive layer on the fabric surface.

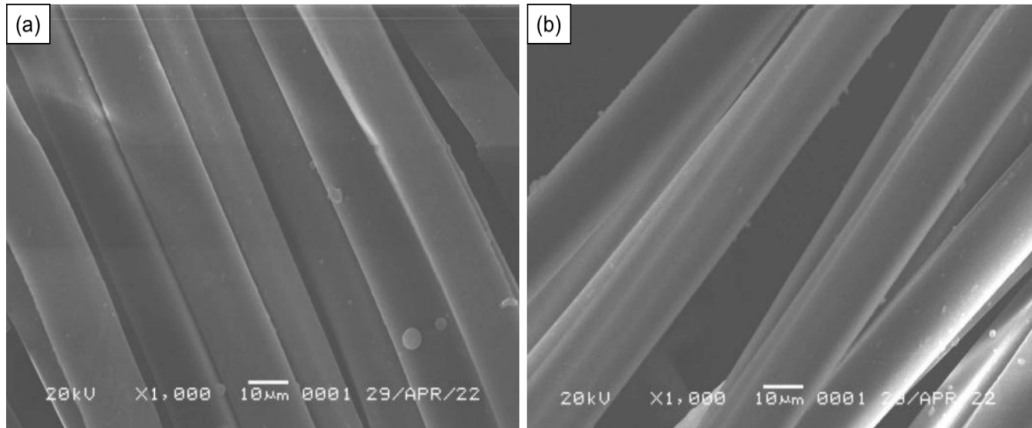


Fig. 2. Before and after plasma treatment of warp-knitted fabric. (a) Untreated warp-knitted fabric. (b) Plasma-treated warp-knitted fabric

It is beneficial to improve its wear resistance and durability.

Therefore, to improve the durability of the PANI conductive layer, the fabric is first treated by plasma. The specific processes are as follows:

(1) Plasma treatment: The warp-knitted fabric is cut to 20 cm×20 cm and placed in an SY-DT03S low-temperature plasma processor (Suzhou Opus Plasma Technology Co., LTD.) for pre-treatment to increase the absorption of PANI, as shown in Figure 2(a). The plasma treatment parameters are as follows: air atmosphere, pressure 40 Pa, discharge power 90 W, and treatment time 90 s.

Figure 2(b) shows the surface morphology of Dacron fiber before and after plasma treatment. As illustrated in the figure, before plasma treatment, the surface of the polyester fiber is smooth and flat, but after plasma treatment, the fiber surface is uneven, and the roughness is greatly improved. This is mainly caused by the etching effect of high-energy particles in the plasma on the surface of the fiber and by the formation of tiny pits. At the same time, the plasma treatment will introduce numerous polar groups on the fiber surface. The introduction of polar groups and the improvement of fiber surface roughness greatly improve the surface energy of the fiber, which is conducive to improving the adsorption fastness and uniformity of polyester fiber to PANI.

(2) Appropriate PVA particles are weighed and placed in a three-mouth flask filled with 90°C deionized water and mechanically stirred in a constant temperature water bath until they are completely dissolved. After the solution is cooled, An monomer is added and mixed solution A containing PVA and An is prepared. The mass ratio of PVA to An in the mixed solution is 0.00%, 1.00%, 4.00% and 8.00%.

(3) The plasma-treated fabric is immersed in mixed solution A for 2 hours and is then removed. Then the fabric is extruded and weighed by a rolling mill several times. The mass ratio of the warp-knitted fabric and adsorbed mixed solution is controlled to be 1:1.

Subsequently, mixed solution B containing the doped acid and oxidant is prepared, in which the concentration of the doped acid HCl is 0.7 mol/L and that of the oxidant air plasma spray (APS) – 35 g/L. According to the ratio of 1 g mixed solution A to 100 ml mixed solution B adsorbed on the fabric, the fabric is immersed in mixed solution B and then placed in a constant temperature water bath oscillator. The mixed solution is shaken at a water temperature of 25°C for 2 hours so that it can fully and evenly react. After the reaction, the fabric is washed with deionized water. Finally, the fabric is dried at room temperature for 10 hours and then moistened for 24 hours under standard atmospheric conditions. PANI coated conductive warp-knitted fabric (PCCWKF) is thus prepared.

2. Experiments to Analyze the Structure and Properties of PCCWKF

2.1. SEM Photo of PCCWKF

After plasma treatment, using the JMS-6360LV (Japanese Electronics Co., LTD) shown in Figure 2, the surface morphologies of the warp-knitted conductive fabric before and after 1000 times of scanning via SEM are obtained.

Figure 2(a) shows that untreated polyester fibers in the warp-knitted fabric display a cylindrical structure and smooth surface. Figure 2(b) shows that after plasma treatment, the fiber surface is generated in parts of the small particles and potholes, and the convex surface roughness increases, which is beneficial for enhancing the surface energy of the fiber and improving the adhesion fastness to the PANI conductive layer.

A conductive layer of PANI is formed on the surface of the fabric after conductive treatment, and its structure changes greatly. The mass ratios of PVA to An in the mixed solution are 0.00%, 1.00%, 4.00% and 8.00%, shown in Table 2.

As shown in Table 2(a), when the conductive layer does not contain PVA, the surface structure uniformity of the yarn is poor, and obvious agglomerated PANI can be seen. Table 2(b) shows that when the mass ratio of PVA to An gradually increases in the mixed solution, PANI that reunited on the surface of the

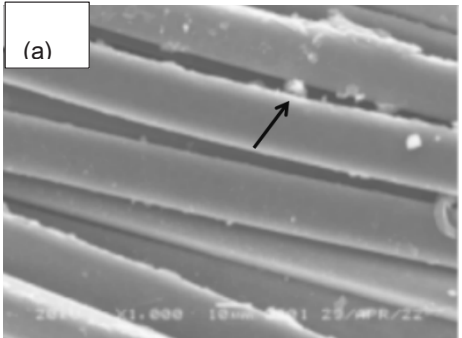
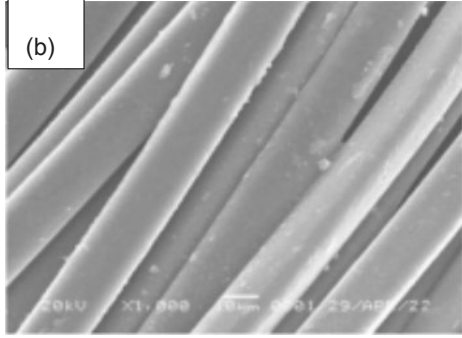
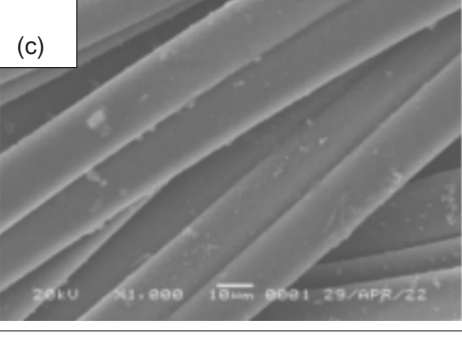
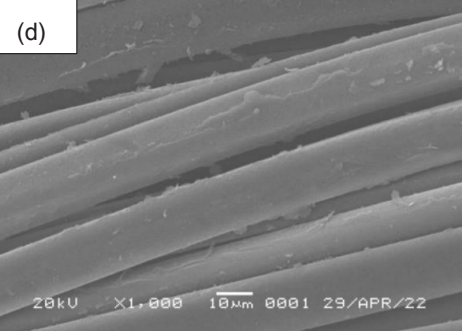
Samples	Mass ratio of PVA to An	SEM at 1000 magnification
PCCWKF-1	0% When the conductive layer does not contain PVA, obvious agglomerated PANI can be seen	
PCCWKF-2	1%	
PCCWKF-3	4% The large size particles and aggregates on the surface of yarn basically disappear	
PCCWKF-4	8% As the mass ratio of PVA to An continues to increase, the yarn surface roughness gradually increases	

Table 2. Topographic external appearance of PCCWKF with different concentrations

yarn size presents a downward trend. When the mass ratio of PVA to An reaches 4%, as shown in Table 2(c), large-size particles on the surface of the yarn and agglomerate disappear. The conductive surface becomes smooth and the yarn is completely coated. As the mass ratio of PVA to An continues to increase, the yarn surface roughness gradually increases, as

shown in Table 2(d). The analysis above shows that the addition of the appropriate amount of PVA can help PANI form a stable interpenetrating polymer network structure and improve its uniformity; but excessive PVA has a negative effect on the uniformity of the PANI structure [6].

2.2. Sensing Property Analysis of PCCWKF

Table 3 shows four different concentrations of PCCWKF, namely, the conductive warp-knitted fabric without PVA (PCCWKF-1), the conductive warp-knitted fabric with the least amount of PVA (PCCWKF-2), the conductive warp-

knitted fabric with the most conductive ability (PCCWKF-3), and the conductive fabric with the greatest amount of PVA (PCCWKF-4).

There is no obvious difference in the appearance of the fabric, but due to the coating of the conductive layer, the color of the fabric appears dark green, and the color deepens as the concentration increases.

The following four conductive warp-knitted fabrics, PCCWKF-1, PCCWKF-2, PCCWKF-3 and PCCWKF-4, were tested to detect their resistance changes under different

tension–recovery states and analyze their strain–resistance sensing performance.

The conductive warp-knitted fabric is stretched in a reciprocating manner. Figures 3–6 show the resistance variation of the four conductive fabrics under the action of 10% tensile recovery. The ac segment is the fabric stretching stage, at which the resistance shows a downward trend, while the cd segment is the fabric recovery stage, at which the resistance shows an increasing trend. Notably, the resistance variation trend of PCCWKF-1, PCCWKF-2, PCCWKF-3 and PCCWKF-4 is exactly the same under reciprocating stretching.

As seen from Figures 3-6, the stretching stages of PCCWKF-1, PCCWKF-2, PCCWKF-3 and PCCWKF-4 are illustrated. In the stretching phase of the four diagrams above, the findings indicate that the resistance changes present two different phases. In particular, the ac stage presents a downward trend, but in the initial stage of ab, the resistance changes slowly and a small amount of improvement can be seen, while the bc stage has a more obvious downward trend than the ab stage. Additionally, the characteristic of the resistance varying in stages is related to the structure of the double-warp fabric.

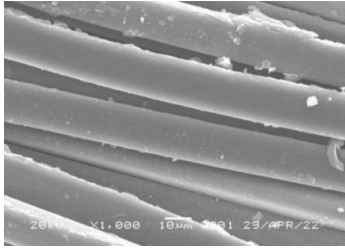

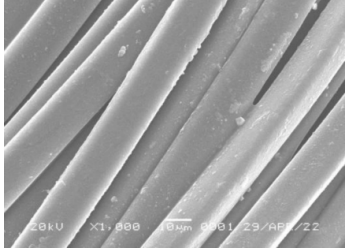

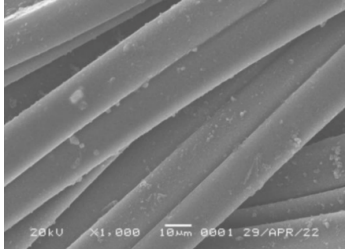

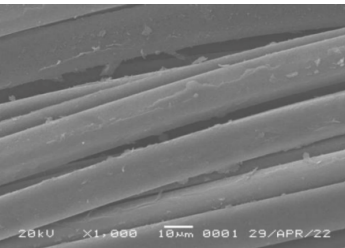

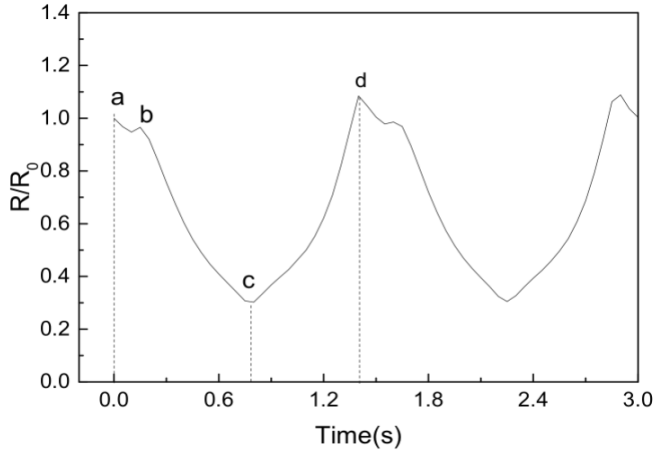
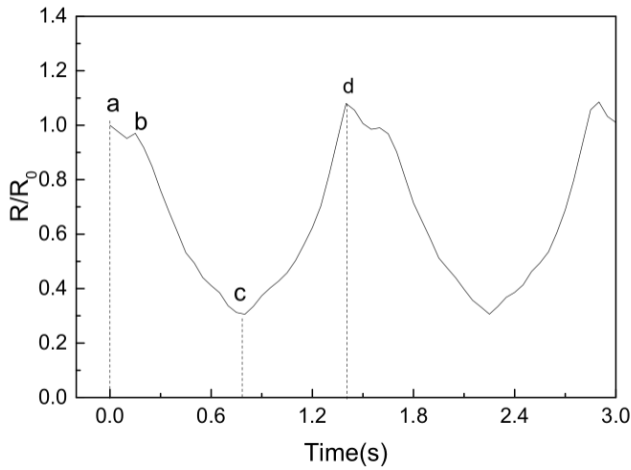
Sample	Mass ratio of PVA to An /%	HCl concentration/ molmol·L ⁻¹	APS concentration /g·L ⁻¹	SEM	Figure
PCCWKF-1	0	0.7	35		
PCCWKF-2	1				
PCCWKF-3	4				
PCCWKF-4	8				

Table 3. PCCWKF sensor appearance



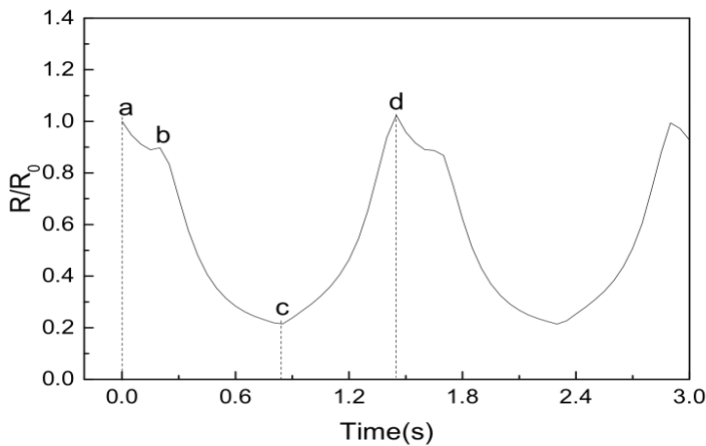
(a) PCCWKF-1

Fig. 3. Resistance variation of (a) PCCWKF-1 at a strain of 10%



(b) PCCWKF-2

Fig. 4. Resistance variation of (b) PCCWKF-2 at a strain of 10%



(c) PCCWKF-4

Fig. 5. Resistance variation of (c) PCCWKF-4 at a strain of 10%

Figure 7(a) is the structural model of two-bar tricot fabric. When the voltage is applied horizontally along the fabric, the resulting resistance network model of the fabric is illustrated in Figure 7(b), where R_C is the contact resistance generated by the contact between the upper and lower coils, and R_L is the length resistance of the coil extension line itself. When the fabric is stretched horizontally, the dry part of the ring is tightened and shortened, and the extension line is extended, resulting in an increase in R_L . However, due to the special structure inherent in the double-warp flat structure, the extension range of the extension line is small, hence the space for the increase in R_L is small. On the other hand, when the fabric is stretched horizontally, the fabric becomes wider, which widens the connecting part between the upper and lower coils, resulting in an increase in the contact area, thus reducing the contact resistance. At the same time, the transverse stretching also leads to an increase in the contact force between the upper and lower coils, and the relationship between the contact force and contact resistance is satisfied by

$$R_C = K F_C^{-m} \quad (1)$$

(where F_C is the contact force, and K and m are the constants related to the material and the contact state, respectively). Notably, with an increase in the contact force, the contact resistance R_C decreases as a power function.

According to the analysis above, at the initial stage of transverse stretching, the resistance of the conductive warp-knitted fabric increases due to the elongation of the extension line and decreases due to the increase in the contact area and contact force. The former offsets part of the effect of the latter, resulting in a relatively slow resistance change. However, after the initial stage of stretching, the length of the extended line is basically unchanged, and the resistance is mainly affected by the latter. Therefore, the resistance decreases significantly, and the strain-resistance sensor sensitivity is higher than that of the initial stage.

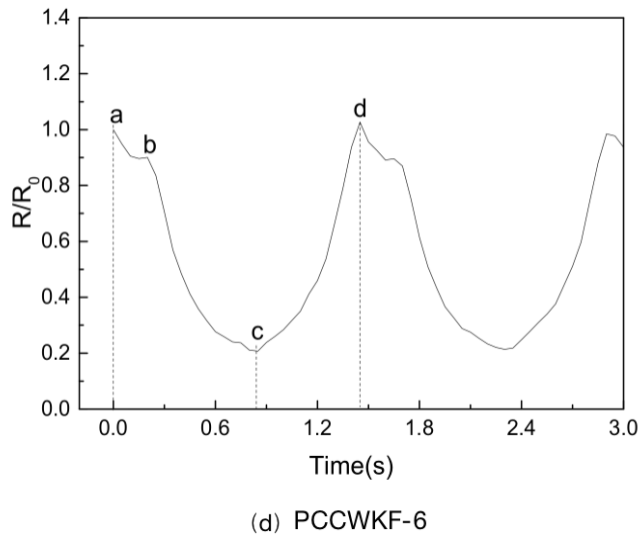


Fig. 6. Resistance variation of (d) PCCWKF-6 at a strain of 10%

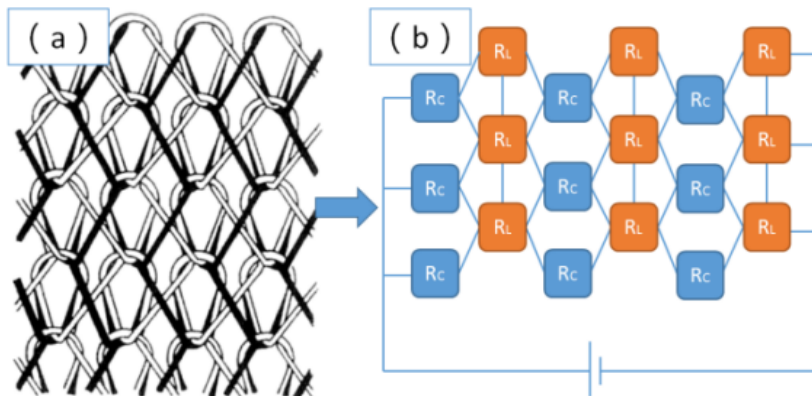


Fig. 7. Picture of network model of two bar tricot fabric. (a) Structure. (b) Resistance

To understand the resistance variation of the conductive warp-knitted fabrics under different strains and multiple tensile recoveries, namely, the repeatability of the sensing properties, the four conductive fabrics, PCCWKF-1 and PCCWKF-2, PCCWKF-3 and PCCWKF-4, are reciprocated and stretched for a long time. The results are shown in Figure 8.

Figure 8 shows the resistance variation of the four conductive warp-knitted fabrics at a strain of 5%, where (a), (b), (c) and (d) are the changes in the resistance of PCCWKF-1, PCCWKF-2, PCCWKF-3 and PCCWKF-4 under the action of a long-time reciprocating stretch of 1000 s, respectively. Each small figure shows four kinds of conductive warp-knitted fabrics at 0-10 s. Details of the resistance

changes between different time periods of 495~505 s and 990~1000 s are shown.

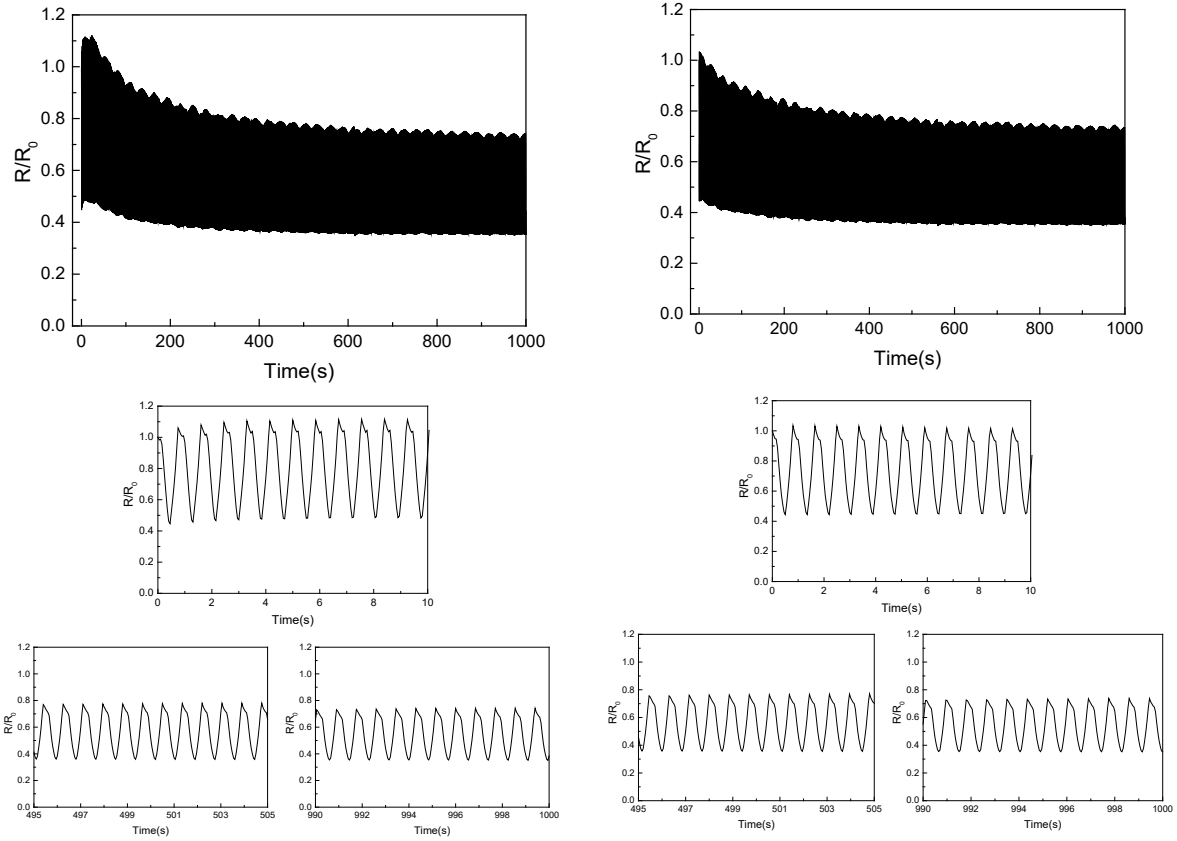
As seen from Figures 8, at a strain of 5%, the resistance of PCCWKF-1, PCCWKF-2, PCCWKF-3 and PCCWKF-4 all show a trend of decreasing gradually with the progress of stretching and then becoming stable. At the initial stretch, the highest R/R_0 of PCCWKF-1 was 1, which showed a slow increasing trend in the early stage and then decreased continuously. At approximately 200 s, the highest R/R_0 value of PCCWKF-1 decreased from the initial 1 to approximately 0.84, and the lowest R/R_0 value decreased from the initial 0.5 to approximately 0.4 and remained stable. At a strain of 5%, the variation trends of PCCWKF-2, PCCWKF-3 and PCCWKF-4 were

similar to that of PCCWKF-1. After 200 s of reciprocating stretch, the highest and lowest R/R_0 values of PCCWKF-2 decreased from approximately 1 and 0.56 to approximately 0.81 and 0.37, respectively. The highest and lowest R/R_0 values of PCCWKF-3 decreased to approximately 0.88 and 0.49, respectively, and the highest and lowest R/R_0 values of PCCWKF-4 decreased to approximately 0.90 and 0.59, respectively, and remained stable for a long time. This phenomenon, illustrating that the resistance gradually decreases and then tends to maintain stability with the stretch, occurs because the contact between the conductive fabric coils becomes closer after several stretches, which leads to a decrease in the contact resistance.

According to Figures 8, equations are used to calculate the sensing sensitivity of PCCWKF-1, PCCWKF-2, PCCWKF-3 and PCCWKF-4 at different time periods under the condition of 5% strain. The four tables reveal that the sensitivity of different samples showed a similar pattern; that is, the sensitivity gradually decreased with the prolongation of time. The results are shown in Tables 4-7. For example, the average sensitivity of PCCWKF-1 is 11.31 at 0-10 s, but those of 10.72 and 10.40 occur at 495-505 s and 990-1000 s, respectively.

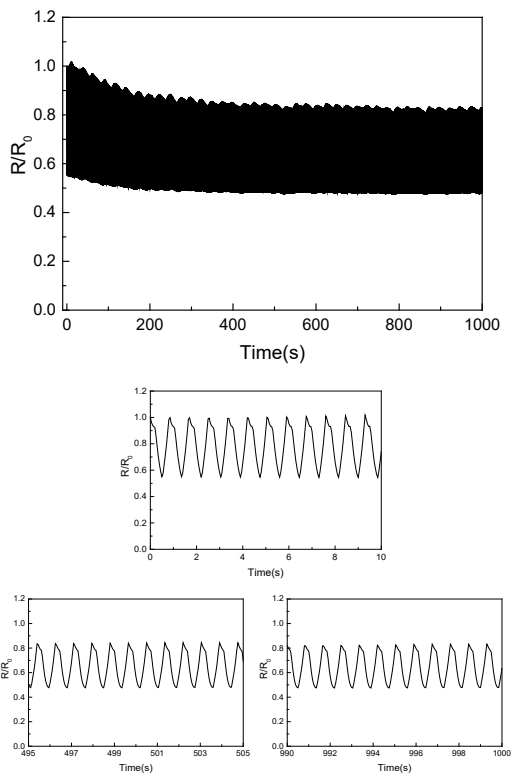
At the same time, the comparison of the sensitivities of the four conductive warp-knitted fabrics horizontally indicates that the sensitivity of PCCWKF-1 is the highest, while the sensitivities of PCCWKF-2, PCCWKF-3 and PCCWKF-4 gradually decrease, indicating that the addition of PVA has an adverse effect on the sensitivity of the sensor.

Notably, the higher the content of PVA is, the lower the sensitivity of the sensor. Therefore, based on the electrical conductivity, mechanical properties, wearability and sensitivity of the fabrics, only PCCWKF-1 and PCCWKF-3 were used for the subsequent sensing performance tests of different conductive warp-knitted fabrics at different elongation rates.

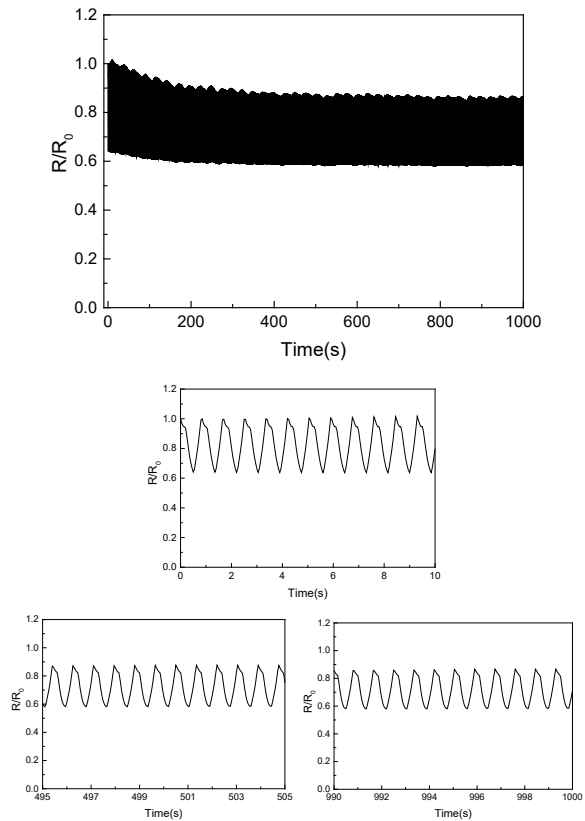


(a) PCCWKF-1

(b) PCCWKF-2



(c) PCCWKF-3



(d) PCCWKF-4

Fig. 8. Repeatability of strain-resistance sensing of (a) PCCWKF-1, (b) PCCWKF-2, (c) PCCWKF-3 and (d) PCCWKF-4 at 5% strain

Period	Cycle	Highest value of R/R0	Lowest value of R/R0	GF	Average value of GF
0~10 s	1	1	0.44704	11.059	11.31
	2	1.05976	0.45693	11.377	
	3	1.07945	0.46647	11.357	
	4	1.0951	0.47136	11.391	
	5	1.10503	0.47563	11.392	
	6	1.10406	0.47768	11.347	
	7	1.1099	0.48133	11.327	
	8	1.10795	0.48392	11.265	
	9	1.11317	0.48491	11.288	
	10	1.11515	0.48541	11.294	
495~505 s	1	0.76909	0.36092	10.614	10.72
	2	0.77034	0.36026	10.647	
	3	0.77066	0.35975	10.664	
	4	0.77382	0.36002	10.695	
	5	0.77413	0.35913	10.722	
	6	0.7762	0.35855	10.761	
	7	0.77668	0.35879	10.761	
	8	0.77812	0.35866	10.781	
	9	0.77876	0.35842	10.795	
	10	0.7786	0.35801	10.804	
990~1000 s	1	0.73014	0.35418	10.298	10.40
	2	0.73113	0.35375	10.323	
	3	0.73283	0.35402	10.338	
	4	0.73597	0.35478	10.359	
	5	0.73784	0.35468	10.386	
	6	0.74015	0.35455	10.420	
	7	0.74102	0.35388	10.449	
	8	0.74059	0.35349	10.454	
	9	0.74175	0.35302	10.481	
	10	0.74132	0.35263	10.486	

Table 4. Sensitivity of PCCWKF-1 at different time periods (5%)
The sensitivities of PCCWKF-2 are 11.52, 8.07 and 7.53.

According to the analysis in Figures 8,, the addition of PVA has little influence on the sensing performance of PCCWKF under the condition of a 5% small strain, and both PCCWKF-1 and PCCWKF-3 have good and stable strain-resistance sensing performance. However, with an increase in the strain, the addition of PVA contributes to the improvement of the flexibility of the PANI conductive layer, which keeps its structural integrity in the reciprocating stretch–recovery cycle, and thus keeps its strain-resistance sensing performance stable. Furthermore, the larger the strain is, the more obvious the contribution.

3. Experiment of Motion Monitoring for seniors

The content of this pre-experiment was developed with PCCWKF-3 as the sensor for motion monitoring, placed on the subject's chest, elbow and knee, to conduct a motion monitoring experiment. The structure and performance of the four PCCWKF sensors were tested and analyzed in a number of experiments. Furthermore, when the mass ratio of PVA to An reached 4%, the large-size particles and aggregates on the yarn surface basically disappeared, the conductive layer became smooth, and the yarn was completely covered. Notably, when the

mass ratio of PVA to An reaches 4%, PVA helps to improve the conductivity of the PANI conductive layer on the fabric surface, and its resistivity is the best. Respiratory assessment was also included in the motion monitoring experiment. Since respiration is used in the course of clinical treatment, monitoring the safety and health of seniors uses this as a reference. However, in actual daily life, it is difficult to have a simple and reliable respiratory monitoring method suitable for the home and clinic. Respiration is an important physiological parameter to characterize the health of the human body. According to the frequency and depth of breathing, the recovery of some diseases

Period	Cycle	Highest value of R/R0	Lowest value of R/R0	GF	Average value of GF
0~10 s	1	1	0.44499	11.100	11.52
	2	1.03401	0.44473	11.786	
	3	1.03231	0.44462	11.754	
	4	1.02977	0.44615	11.672	
	5	1.02921	0.44673	11.650	
	6	1.02753	0.44721	11.606	
	7	1.02501	0.44769	11.546	
	8	1.02029	0.44881	11.430	
	9	1.01864	0.45031	11.367	
	10	1.01727	0.45155	11.314	
495~505 s	1	0.75657	0.35792	7.973	8.07
	2	0.75626	0.35816	7.962	
	3	0.76008	0.35799	8.042	
	4	0.74462	0.35761	7.740	
	5	0.76269	0.35732	8.107	
	6	0.76377	0.35674	8.141	
	7	0.76424	0.35647	8.155	
	8	0.76486	0.35603	8.177	
	9	0.76625	0.35593	8.206	
	10	0.76813	0.3561	8.241	
990~1000 s	1	0.72278	0.35486	7.358	7.53
	2	0.72556	0.35489	7.413	
	3	0.72696	0.35435	7.452	
	4	0.72752	0.35425	7.465	
	5	0.72991	0.35415	7.515	
	6	0.7319	0.35405	7.557	
	7	0.73289	0.35349	7.588	
	8	0.73361	0.35302	7.612	
	9	0.73532	0.35352	7.636	
	10	0.73719	0.35289	7.686	

Table 5. Sensitivity of PCCWKF-2 at different time periods (5%)
The sensitivities of PCCWKF-3 are 9.05, 8.62 and 8.46.

can be reflected. Therefore, respiration was taken as the pre-experiment in the motion monitoring experiment. As the test purpose of this pre-experiment was to determine whether the sensor appropriately performs the monitoring function, there was no special population setting for the test object. The object of this pre-experiment was a young woman.

3.1. Fabrication of the Sensor

As shown in Figure 9, a conductive adhesive is applied to the metal buckle at

both ends of the PCCWKF-4 embedded in the lining of the garment. This approach holds the wire in place so that it is in close contact with the fabric to ensure that its current can be transmitted stably. Figure 10 is the visual effect of making PCCWKF on the waist in sportswear.

In the pre-experiment of motion monitoring, the selections of respiration and elbow and knee joints were elaborated, and these three motions were employed to perform monitoring. To ensure the consistency of the experiment, the respiration, elbow and knee motions

were still tested in this experiment of smart clothing for motion monitoring of seniors.

3.2. Respiratory Monitoring

As shown in Figure 9, the electrode cable shown in Figure 9(c) on both sides of the sensor is connected to the electrochemical workstation shown in Figure 9(a) through the metal joint shown in Figure 9(b) by the subject wearing a sports bra. The changes in the resistance of the sensor were recorded during respiration in three

Period	Cycle	Highest value of R/R0	Lowest value of R/R0	GF	Average value of GF
0~10 s	1	1	0.55113	8.977	9.05
	2	0.99838	0.55019	8.978	
	3	0.99717	0.54946	8.980	
	4	0.9945	0.54832	8.973	
	5	0.9933	0.54767	8.973	
	6	0.99731	0.54711	9.028	
	7	1.00094	0.54642	9.082	
	8	1.00366	0.54561	9.128	
	9	1.00638	0.54541	9.161	
	10	1.0094	0.54541	9.193	
495~505 s	1	0.83483	0.47745	8.562	8.62
	2	0.83596	0.47717	8.584	
	3	0.83738	0.47686	8.611	
	4	0.83833	0.47662	8.629	
	5	0.83928	0.47668	8.641	
	6	0.84042	0.47736	8.640	
	7	0.84223	0.47822	8.644	
	8	0.84358	0.47902	8.643	
	9	0.84406	0.47973	8.633	
	10	0.84396	0.48045	8.614	
990~1000 s	1	0.81915	0.47546	8.391	8.46
	2	0.81951	0.47491	8.410	
	3	0.82087	0.47457	8.437	
	4	0.82233	0.47454	8.459	
	5	0.8237	0.47482	8.471	
	6	0.82609	0.47579	8.481	
	7	0.82886	0.47683	8.494	
	8	0.831	0.47785	8.499	
	9	0.83193	0.4784	8.499	
	10	0.83174	0.47902	8.481	

Table 6. Sensitivity of PCCWKF-3 at different time periods (5%)
The sensitivities of PCCWKF-4 are 7.28, 5.81 and 5.61.

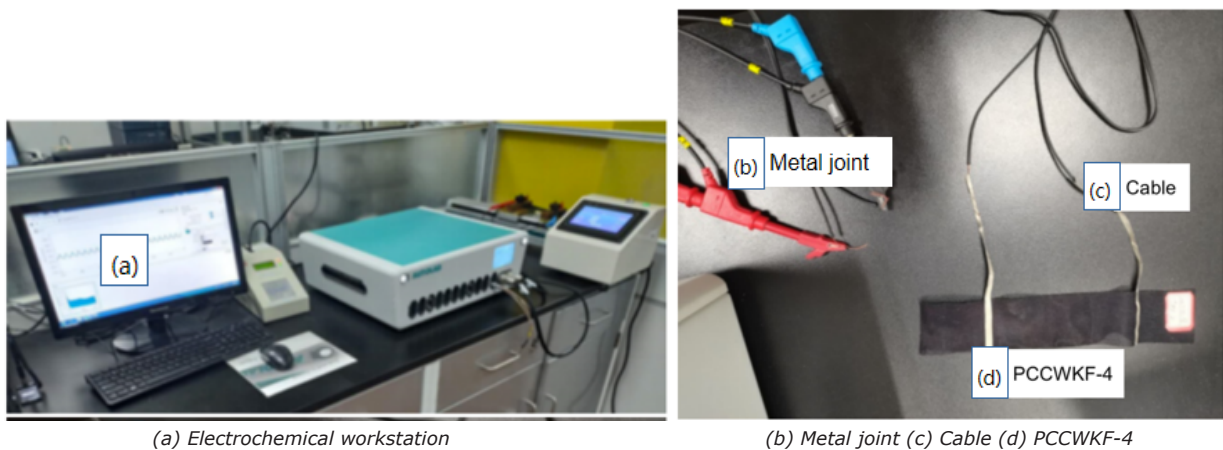


Fig. 9. Fabric sensor

Period	Cycle	Highest value of R/R0	Lowest value of R/R0	GF	Average value of GF
0~10 s	1	1	0.64098	7.180	7.28
	2	0.99903	0.6404	7.173	
	3	0.99689	0.63948	7.148	
	4	0.99593	0.63896	7.139	
	5	0.99914	0.63852	7.212	
	6	1.00205	0.63796	7.282	
	7	1.00423	0.63731	7.338	
	8	1.00641	0.63715	7.385	
	9	1.00883	0.63715	7.434	
	10	1.01114	0.63731	7.477	
495~505 s	1	0.8699	0.58249	5.748	5.81
	2	0.87103	0.58224	5.776	
	3	0.87179	0.58205	5.795	
	4	0.87255	0.5821	5.809	
	5	0.87347	0.58264	5.817	
	6	0.87492	0.58333	5.832	
	7	0.876	0.58397	5.841	
	8	0.87638	0.58454	5.837	
	9	0.8763	0.58512	5.824	
	10	0.876	0.58552	5.810	
990~1000 s	1	0.85672	0.58068	5.521	5.61
	2	0.85781	0.58041	5.548	
	3	0.85898	0.58038	5.572	
	4	0.86007	0.58061	5.589	
	5	0.86199	0.58139	5.612	
	6	0.86421	0.58222	5.640	
	7	0.86592	0.58304	5.658	
	8	0.86667	0.58348	5.664	
	9	0.86652	0.58397	5.651	
	10	0.86637	0.58402	5.647	

Table 7. Sensitivity of PCCWKF-4 at different time periods (5%)

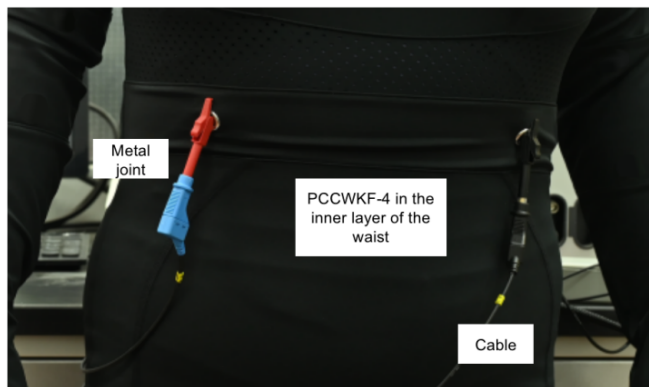


Fig. 10. Sensors on the waist of the clothing

different states, such as sleeping, sitting and running for 5 mins.

Figures 11–12 show the change in resistance of the fabric sensor when the sports bra was worn in different states by the experimenter, such as sleeping, sitting

still and after 5 min of running. A wave peak in the curve represents one breath, and it can be seen that the sensor shows very obvious and regular resistance changes in different exercise states, suitably monitoring the human breathing condition.

According to Table 8, after sleeping, sitting and running for 5 min, the difference between the maximum and minimum R/R0 values is 0.014, 0.035 and 0.140, respectively, indicating that the elongation and deformation of sportswear during breathing are different under various exercise states; that is, the fluctuation state of the abdominal cavity is different. The fluctuation of the abdominal cavity during sleep is the smallest, while that during exercise is the largest. At the same time, the breathing rate of the human body is also different in different exercise states. This indicates that the conductive warp-knitted fabric sensor can not only record the occurrence of respiration but also monitor the respiratory rate and respiratory intensity, indicating that the sports bra detects the different motion states of the worn object.

Table 8. Data of respiration monitoring

Movement status	Difference between the maximum and minimum values of R/R ₀	Respiratory interval/s
Sleeping	0.014	3.01
Sitting	0.035	2.84
Running for 5 min	0.140	3.97

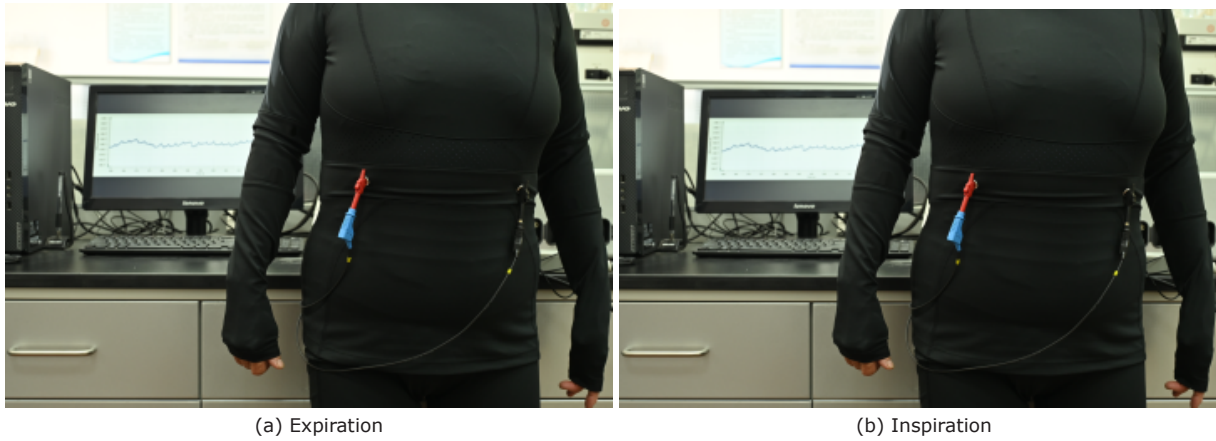
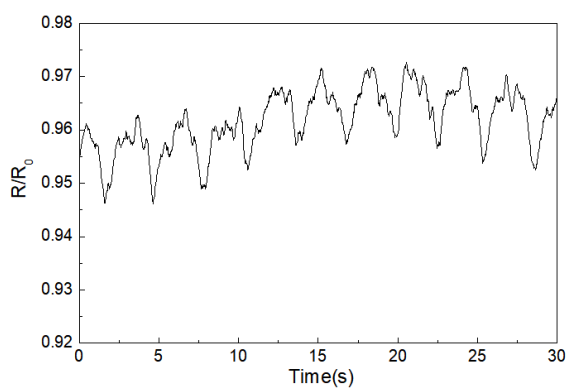
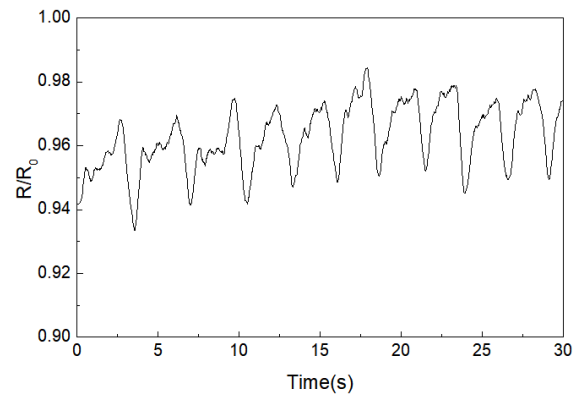


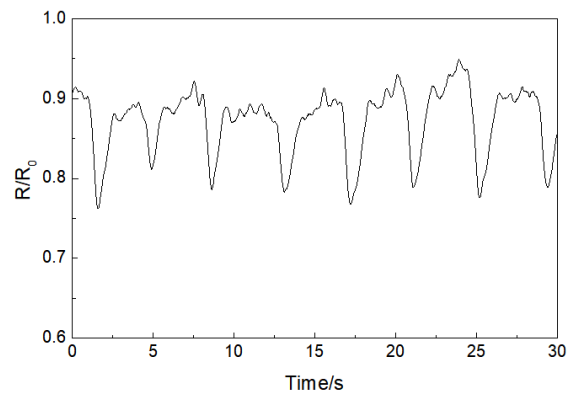
Fig. 11. Respiration monitoring experiment



(a) Resistance variation of sensor during sleeping



(b) Resistance variation of sensor during sitting



(c) Resistance variation of sensor during running for 5 mins

Fig. 12. Resistance variation of sensor of during sleeing, sitting and running for 5 mins

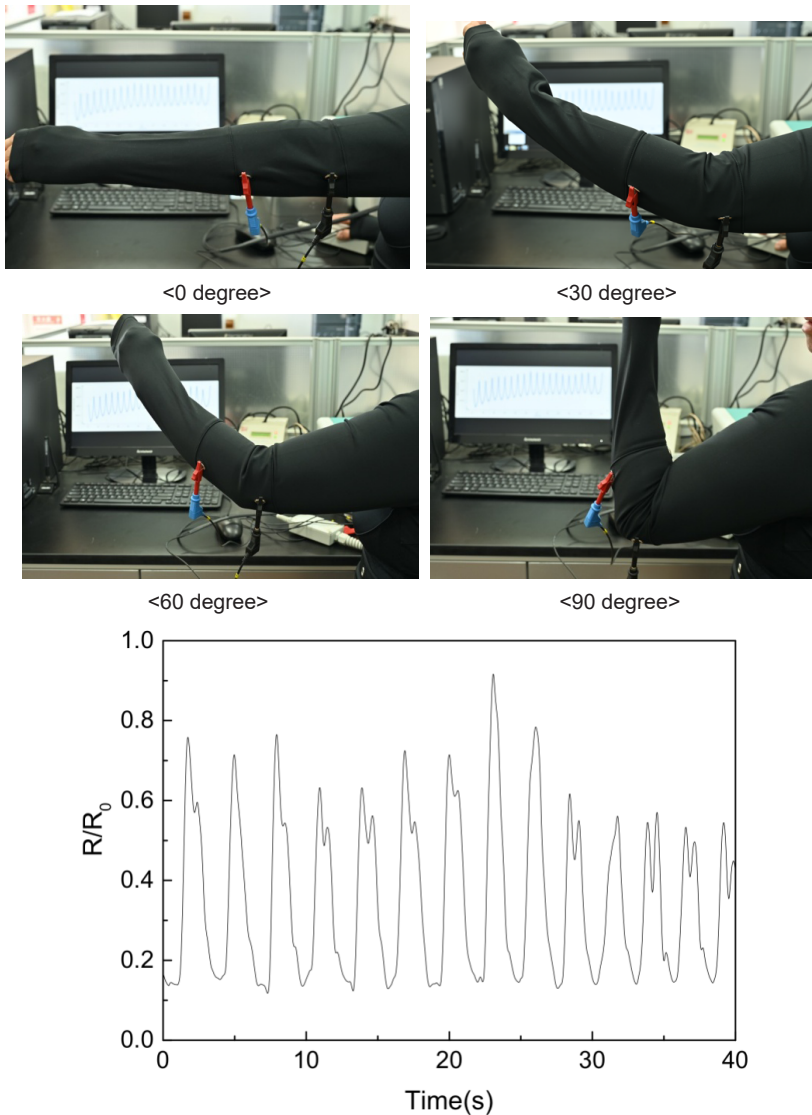


Fig. 13. Resistance variation of the sensor elbow motion monitoring at 0, 30, 60, 90 degrees

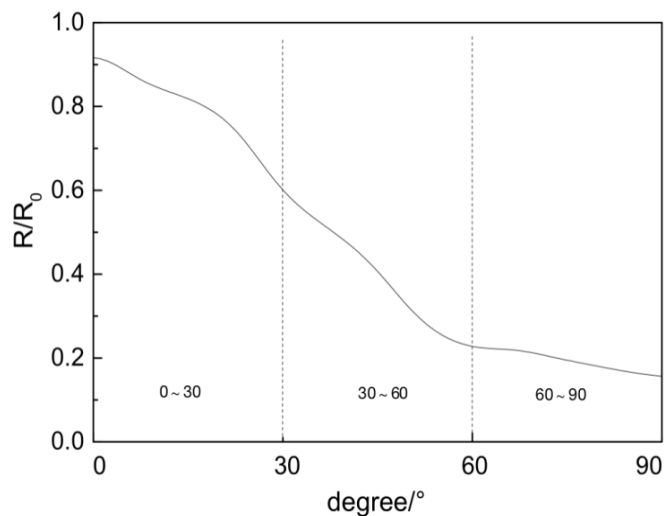


Fig. 14. Resistance variation of the elbow motion monitoring sensor in one cycle at 0, 30, 60, and 90 degrees in the pre-experiment

3.3. Elbow Motion Monitoring

As shown in Figure 18, the fabric is tightly fitted to the elbow of the human body and fixed for the continuous bending experiment. In the continuous bending experiment, the changes of the current with time during continuous bending of the elbow were recorded in real time.

Figures 13–14 show the relative resistance–time curve when the elbow is continuously bent. When the angle from bending the elbow in the range 0° – 90° shifts, the resistance of the fabric decreases with the increase of the stretching length. When the elbow bends to 90° , the fabric stretches to the maximum degree and the fabric resistance reaches the minimum value. Then, the motion of the small part of the arm makes the angle shift from 90° – 0° ; the fabric begins to respond, and the resistance starts to increase. Since each elbow motion of the human body has a certain deviation and the fabric is undergoing a stretching and response process, the resistance change has a certain fluctuation. However, the elbow motion in the images for each cycle can be clearly distinguished, and a certain similarity can be observed.

3.4. Knee Motion Monitoring

As shown in Figure 15, the fabric was tightly laminated to the knee area by a specific method, fixed and then tested for the change in current generated during walking and running. In addition, the change in current over time was recorded in real time.

The position of each trough of the curve in the figure indicates the maximum moment of right knee flexion—the point at which the fabric stretches to its maximum position. The fabric takes one step for each of the right and left feet throughout the stretch to recovery, i.e., a total of two steps in a single cycle of resistance change. The time period when the resistance is more stable during walking is selected in Figures 15–17. Notably, the current gradually changes as the knee bends, and the trend of change is more regular.

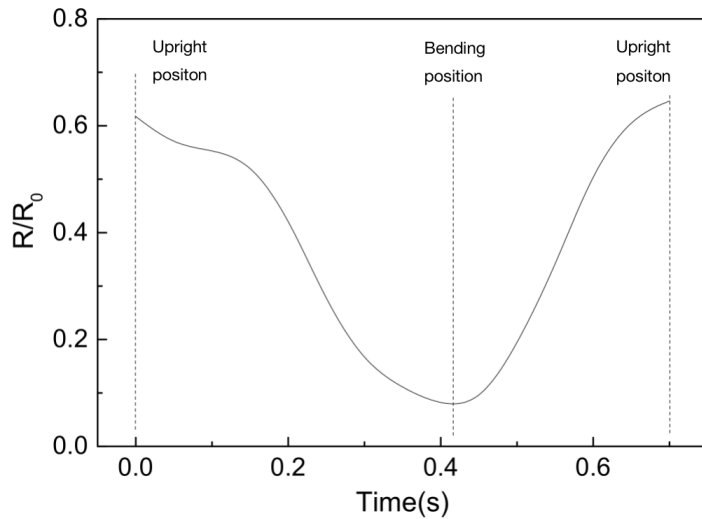


Fig. 15. Resistance variation of the knee motion monitoring sensor in one cycle of the pre-experiment

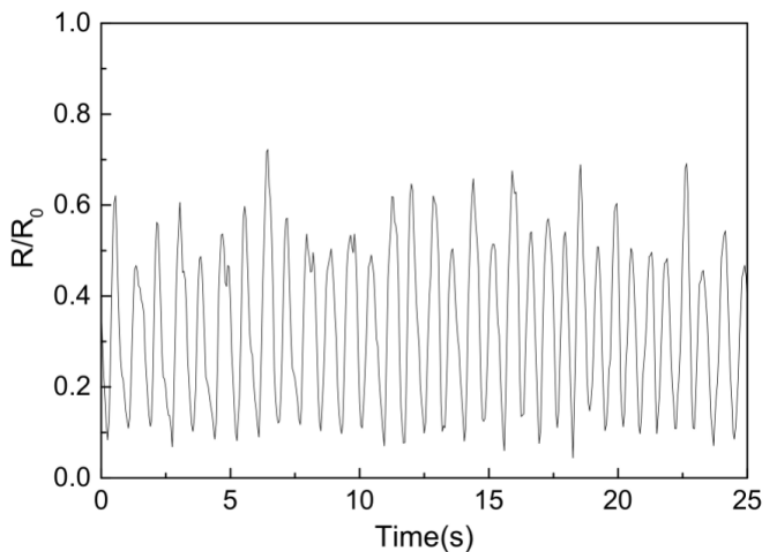
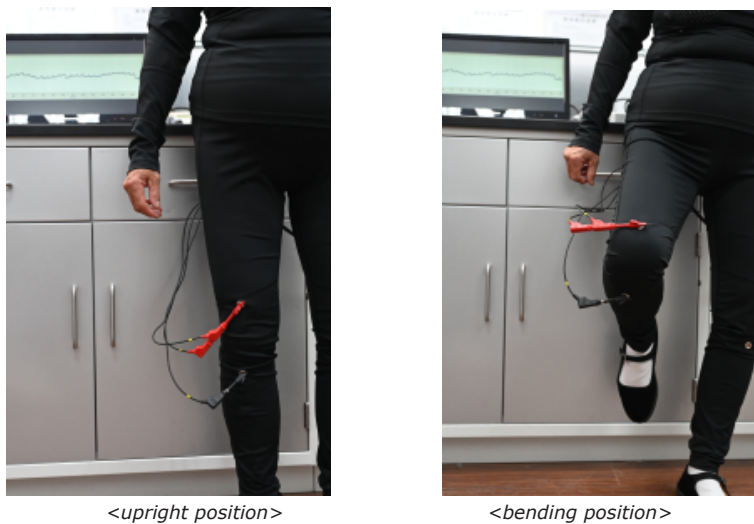


Fig. 16. Resistance variation of the knee motion monitoring sensor

4. Conclusions

In this paper, the double-warp-knitted flat structure of a warp-knitted fabric was used as the base material. PANI conductive warp-knitted fabrics were prepared by plasma treatment and in-situ polymerization. PVA was used as a toughening material to improve the flexibility of the PANI conductive layer on the PCCWKF surface, thereby improving its electrical resistance and durability. The structure and properties of PCCWKF were tested and analyzed, as well as the strain sensing performance of PCCWKF under different tensile states. The following conclusions are drawn:

(1) Scanning electron microscopy shows that after plasma treatment, some raised small particles and pits are generated on the fiber surface of the warp-knitted fabric, and the surface roughness is improved, which is conducive to enhancing the surface energy of the fiber and improving the adhesion fastness to the PANI conductive layer. After conductive treatment, a PANI conductive layer was generated on the surface of the fabric fiber. The addition of an appropriate amount of PVA helped PANI to form a stable interpenetrating polymer network structure and improve its uniformity. However, excessive PVA has a negative effect on the uniformity of the structure.

(2) In-situ polymerization on the surface of warp-knitted fabrics generated by adhesion is accomplished with PANI, which endows it with a certain electrical conductivity. The addition of PVA in the in-situ polymerization reaction system can change the electrical conductivity of PANI. With the increase of the content, the resistivity of PCCWKF decreases first and then increases. When the mass ratio of PVA to An increases from 0 to 4.00%, the resistivity decreases from $(1.25 \pm 0.14) \Omega \text{ cm}$ to $(0.82 \pm 0.1) \Omega \text{ cm}$. When the mass ratio of PVA to An increases to 8.00%, the conductivity of the composite conductive yarn increases to $(1.54 \pm 0.21) \Omega \cdot \text{cm}$. This indicates that in a certain range, PVA is helpful in improving the conductivity of PANI, but when the concentration is large, PVA, in

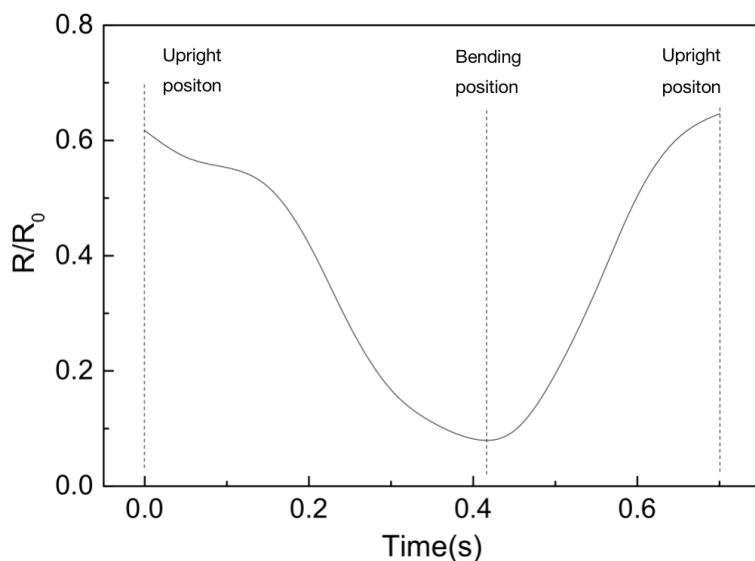


Fig. 17. Resistance variation of the knee motion monitoring sensor in one cycle of the pre-experiment

turn, affects the conductivity of the PANI conductive layer.

(3) The thermal stability of the warp-knitted fabric and its composite system was reduced by the presence of PANI after in-situ polymerization and conduction treatment, but the change is not significant. After in-situ polymerization, the strength and elongation at the break of the warp-knitted fabrics exhibited little difference

compared with those before treatment, indicating that the conductive treatment had little effect on the mechanical properties of the fabrics. Treated by in-situ polymerization, the PANI conductive layer on the surface of the warp-knitted fabric increased the rigidity of the fabric. Nevertheless, from the perspective of the indicator values, the fabric still retained good softness, and at the same time, an impact on the drape is realized. Overall,

the change is not substantial. The warp-knitted fabric treated with the conductive layer still retained good drapability without diminishing the overall effect of the clothing when used as a part of smart clothing. After the in-situ polymerization and conduction treatment, the air permeability and moisture permeability of the warp-knitted fabric were affected to some extent, but their values are still in a very high range, which is not anticipated to influence the comfort afforded by the warp-knitted fabric when used as a part of the clothing.

(4) The PCCWKF-4 sensor developed can monitor the motion of the elbow, knee and other joint parts, as well as the motion amplitude and speed of each joint. Furthermore, placing the sensor in tight-fitting sportswear can realize respiration monitoring, which can not only record the occurrence of respiration but also monitor the respiration frequency and respiration intensity. These findings show that the PCCWKF-4 sensor developed is able to perform monitoring of human joint motion and related physical signs and has noteworthy application prospects in smart clothing.

References

- Feldman, D. (2008). Polymer history. Designed monomers and polymers, 11(1), 1-15.
- Bansal, S., & Raichurkar, P. (2016). Review on the manufacturing processes of polyester-PET and nylon-6 filament yarn. International Journal on Textile Engineering and Processes, 2(3), 23-28.
- Shirakawa, H. (2022). Path to the Synthesis of Polyacetylene Films with Metallic Luster: In Response to Rasmussen's Article. Substantia, 6(1), 121-127.
- Shangyuan. (1991). Development and Progress of Conductive Polymers. Materials Review (12), 13-17.
- Meng, F. (2008). Synthesis and Characterization of Polyaniline Nanofibers. (Master's thesis, Northeastern University). <https://kns.cnki.net/KCMS/detail/detail.aspx?dbname=CMFD2012&filename=2010257039.nh>
- Bhadra, S., Khastgir, D., Singha, N. K., & Lee, J. H. (2009). Progress in preparation, processing and applications of polyaniline. Progress in polymer science, 34(8), 783-810.
- Xiang, H., Deng, N., Zhao, H., Wang, X., Wei, L., Wang, M., Cheng B. & Kang, W. (2021). A review on electronically conducting polymers for lithium-sulfur battery and lithium-selenium battery: Progress and prospects. Journal of Energy Chemistry, 58, 523-556.
- Yue, P., Wang, S., Li, X., & Ge, M. (2014). Preparation of polyaniline/Ag composite conductive fabric via one-step oxidation-reduction reaction. J. Text. Res, 60, 33-42.
- Shao, L., Li, X. Y., & Zhang, X. X. (2014). Preparation of modified aramid/polyaniline composite conductive fiber. J Funct Polym, 27, 302-309.
- Wang, X. H., Tang, Q., Mu, Y. H., & Li, C. Q. (2017). Preparation of PANI-PVA Composite Conductive Coatings Doped with Different Acid. Advances in Polymer Technology, 36(4), 502-506.